NJC

PAPER

Check for updates

Sustainable solutions for removing aged wax-based coatings from cultural heritage: exploiting hydrophobic deep eutectic solvents (DESs)

Chiara Biribicchi, [ID] *[ab] Andrea Macchia,[bc] Gabriele Favero,[d] Romina Strangis,[e] Bartolo Gabriele, [ID] [e] Raffaella Mancuso [ID] [e] and Mauro Francesco La Russa[c]

This study describes the investigation on the use of hydrophobic Deep Eutectic Solvents (DESs) for the removal of nonpolar coatings from works of art to replace toxic solvents. Beeswax and two microcrystalline waxes (R21 and Renaissance®) have been selected as reference nonpolar coatings since they are commonly present in their aged state on metal and stone artifacts. The interaction between the DESs and three waxes has been evaluated through contact angle measurements, solubility tests, and cleaning tests carried out by implementing a method that is ordinarily used by restorers. Tests have been conducted on mockups consisting of microscope glass slides covered by wax. The effective removal of the wax-based coating from the mockups has been assessed through spectrocolorimetry and multispectral imaging under visible (VIS) and ultraviolet light (UV) at 365 nm by loading the waxes with a fluorescent marker (Rhodamine 6G). Fourier Transform Infrared (FT-IR) spectroscopy in the Attenuated Total Reflectance (ATR) mode was performed to assess the presence of both the wax and the solvent on the swabs used for the cleaning tests, confirming the actual interaction among the solvent and the solute. The experimental process proved DESs' potential of being used as green solvents for cleaning treatments on Cultural Heritage.

Introduction

Wax-based protective coatings have been traditionally used to protect both stone and metal sculptures from the erosive action of weather and the corrosive action of rain and atmospheric pollutants such as SO_x, NO_x, CO_2, and chlorides.[1–3] The hydrophobic feature of these materials is one of the main reasons for their persistent use on outdoor metal and stone artworks. Indeed, outdoor bronzes, iron, and lead sculptures undergo corrosion processes that are essentially caused by the presence of water on the artwork's surface resulting from precipitation or condensation and by the washing effect of rainwater.[4–7] On the other hand, the growth of salt crystals within pores is one of the major damage factors in stone weathering and is driven or enhanced by water.[8] Waxes have low water vapor permeability and low gloss, which makes them ideal protective coatings.[9] Formerly, beeswax used to be applied on outdoor stone and metal artifacts.[1,2,7,10,11] The so-called "waxing" process represented a common practice in ancient restoration treatments that allowed for the protection of the artwork from rainfall and atmospheric pollution and sometimes for the toning of the surface.[2] Nowadays, stone and metal sculptures are usually treated with microcrystalline-wax-based protective coatings.[12–14] When it comes to metal artifacts, the coating is typically applied on an acrylic layer to reduce its exposure to the surrounding environment and moisture.[15] This nonpolar coating is considered a "sacrificial layer" able to protect the acrylic one underneath, avoiding its degradation.

Wax coverings tend to degrade over time, making the removal of this layer necessary.[1,16] They tend to embed pollutants and dust due to their low melting point (between 39–65 °C depending on the type of wax), also showing chromatic and morphological alterations.[17] Indeed, even though wax-based coatings are commonly used to protect outdoor sculptures from degradation and are still considered more beneficial maintenance products for outdoor sculptures than most other coatings, their

[a] Department of Earth Sciences, University of Rome La Sapienza, P.le Aldo Moro 5, 00185 Rome, Italy. E-mail: chiara.biribicchi@uniroma1.it

[b] YOCOCU, Youth in Conservation of Cultural Heritage, Via T. Tasso 108, 00185 Rome, Italy. E-mail: andrea.macchia@uniroma1.it

[c] Department of Biology, Ecology and Earth Sciences (DiBEST), University of Calabria, Via Pietro Bucci 12/B, 87036 Arcavacata di Rende, CS, Italy. E-mail: mlarussa@unical.it

[d] Department of Environmental Biology, Sapienza University of Rome, Piazzale Aldo Moro 5, 00185 Rome, Italy. E-mail: gabriele.favero@uniroma1.it

[e] Laboratory of Industrial and Synthetic Organic Chemistry (LISOC), Department of Chemistry and Chemical Technologies, University of Calabria, Via Pietro Bucci 12/C, 87036 Arcavacata di Rende, CS, Italy. E-mail: bartolo.gabriele@unical.it, romina.strangis@unical.it, raffaella.mancuso@unical.it

barrier properties are affected by defects in their structure – namely, where the layer is not consistent – and their vulnerability to chemical alterations induced by weathering.[3,6,18,19] These factors are the main causes of their short lifetime – 2 to 5 years for microcrystalline waxes, which tend to exfoliate and become powdery, thus also altering the aesthetic appearance of the artwork. Indeed, the tendency to deteriorate requires constant maintenance, which means periodic cleaning treatments.[4] For this kind of intervention, hazardous solvents for both the environment and human health are still widely used. Highly flammable and toxic solvents, namely aliphatic and aromatic hydrocarbons, such as Petroleum Ether and White Spirit, are being used due to their physical-chemical properties, even though they are known to cause adverse effects to humans by both inhalation and dermal adsorption.[10,20–24] Their medium-high volatility, low cost, transparency, and purity make them ideal for these applications, while more sustainable low-polar cleaning systems capable to combine the need for the preservation of the artwork's integrity with a greener approach are still lacking.

The role of green chemistry in improving sustainability in the cultural heritage conservation field is increasingly growing.[25,26] The general aim is to replace traditional hazardous methods and products that are still widely used in the field, especially for the removal of aged coatings from artistic surfaces, thus ensuring the safety of both the artworks and the operators.[27–32] Even though a low-impact and effective approach to cleaning treatments is now recognized as an urgent need, novel environmentally friendly solutions and protocols are yet to be investigated. In this framework, Deep Eutectic Solvents (DESs) can be considered promising alternatives to conventional organic solvents due to their excellent physical–chemical properties – *i.e.*, low volatility, high dissolution power, biodegradability, and low toxicity – together with their easy synthesis, accessibility of their natural compounds, low cost, and recyclability.[33] They are mixtures of two or more solid components leading to a strong depression of the melting point when compared to their individual counterparts, due to the presence of nonsymmetric ions with low lattice energy.[34] They form eutectic mixtures of a hydrogen-bonding acceptor (HBA) and a hydrogen-bonding donor (HBD) able to self-associate *via* hydrogen bonds and van der Waals interactions, inducing the charge delocalization responsible for the decrease in the melting point.[35] Hydrophilic DESs can be described by the general formula:

$$Cat^+ \, X^- zY \qquad (1)$$

where Cat^+ represents any ammonium, phosphonium, or sulphonium cation, X is a Lewis base – generally a halide anion – acting as a counter ion, and Y is a Lewis or Brønsted acid of which z molecules interact with the X^- anion.[34] The properties of the final DES are classified based on the nature of the complexing agent and can be adjusted through the selection of the individual components based on their chemical structure and molar ratio.[36,37] The discovery of these non-toxic formulations generated a breakthrough in the world of green chemistry. As eco-friendly solvents, DESs are being used in many areas of science and technology due to their excellent physicochemical properties, such as low volatility and low toxicity. However, although few attempts have been made so far to use hydrophilic DESs in the Cultural Heritage field, hydrophobic DESs have not been yet investigated.[38–41] Hydrophobic DESs can be obtained from a mixture of two components (component A and component B), a hydrogen-bonding acceptor (HBA) and a hydrogen-bonding donor (HBD), generally having no charge. Therefore, they are neutral compounds:[35,42]

$$[\text{Component 1(HBA)-component 2 (HBD)}] \qquad (2)$$
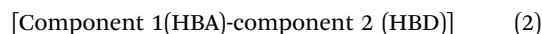
They represent promising solutions, since other potentially suitable compounds that could hypothetically replace aliphatic hydrocarbons come in solid form at room temperature and cannot be used as liquid solvents. Indeed, most of the potential alternatives to toxic solvents consist of molecules having long alkyl chains. As the length of the chain increases, the polarity of the substance decreases, while its melting point increases, making the substance solid at room temperature. The substance's physical state at standard temperatures does not allow for its utilization as a solvent in the liquid form as it needs to be. In this framework, DESs' feature to deeply reduce the melting point value can overcome this limitation and turn low-polar solid substances with medium-long alkyl chains into liquid solvents, while exploiting the solubility properties of their constituents.

The potential of hydrophobic DESs not only relies on the possibility of exploiting the properties of compounds that cannot be used as solvents at room temperature due to their physical state but also on their biocompatibility and low toxicity. These two features are of the outermost importance in the conservation of Cultural Heritage since the operators working on the removal of non-polar coatings are often subjected to inhalation of toxic solvents vapors – *i.e.*, petroleum derivatives – which may cause pathological diseases with long-term exposure.[43] For this reason, we exploited and herein propose for the first time the potential of hydrophobic DESs as new eco-friendly solvents for the removal of low-polar coatings – *i.e.*, waxes – from artistic surfaces, aiming at replacing more hazardous traditional solvents commonly used in the Cultural Heritage sector.
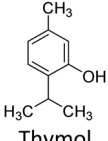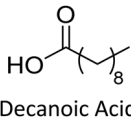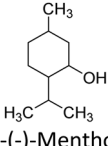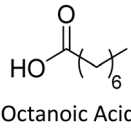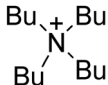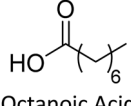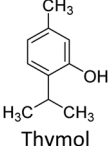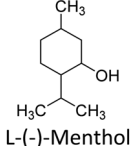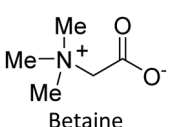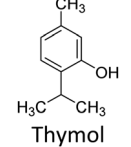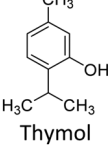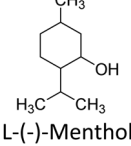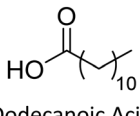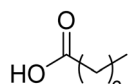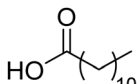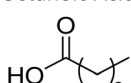
Experimental

Materials and methods

Materials. Beeswax and two microcrystalline waxes that are commonly present as protective coatings on stone and metal sculptures were used. Beeswax and Renaissance® microcrystalline wax polish were purchased from Roma Restauro srl. R21 dispersion of microcrystalline wax in turpentine essence (10% w/v) was purchased from AN.T.A.RES srl. Ligroin 100–140 °C (CAS: 8032-32-4) was provided by I.M.A.R. Italia. Rhodamine 6G (CAS: 989-38-8) was purchased from Sigma-Aldrich®, while dearomatized White Spirit was provided by Antichità Belsito s.r.l. The eight Deep Eutectic Solvents (DES 1 – DES 8) presented in this paper and reported in Table 1 were synthesized

Table 1 Composition of the tested DESs

DES code	Component 1	Component 2	Molar ratio	Melting point [°C]
DES 1	Thymol	Decanoic Acid	1:1[44]	11.5[50]
DES 2	L-(-)-Menthol	Octanoic Acid	1:1[45]	—
DES 3	Tetrabutylammonium	Octanoic Acid	1:1[46]	—
DES 4	Thymol	L-(-)-Menthol	1:2[46]	-4.5[51]
DES 5	Betaine	Thymol	1:3[48]	-15[48]
DES 6	Thymol	L-(-)-Menthol	1:1[47]	—
DES 7	Dodecanoic Acid	Octanoic Acid	1:3[49]	—
DES 8	Dodecanoic Acid	Decanoic Acid	1:2[49]	—

by the Laboratory of Industrial and Synthetic Organic Chemistry (LISOC) within the Department of Chemistry and Chemical Technologies at the University of Calabria. For the synthesis of DESs, Thymol, L-(−)-menthol, tetrabutylammonium bromide, betaine, octanoic acid, decanoic acid, and dodecanoic acid were purchased from Sigma Aldrich (Merck KGaA, Darm-stadt, Germany). Eventually, the only precursor that comes in liquid form at room temperature, namely octanoic acid, was used for the testing as well. With the only exception of DES 3, all the tested solvents consist of compounds of natural origin. Hence, they can be defined as NADES (Natural Deep Eutectic Solvents).

Hydrophobic DESs preparation. Hydrophobic DESs were synthesized by mixing component 1 and component 2 at the proper molar ratio – as shown in Table 1 – and heating them to a temperature between 80 °C and 100 °C until homogeneous liquids were formed in times ranging from 1 to 3 hours.[44–49]

Solubility tests. Solubility tests were performed by mixing 2 parts of wax and 5 parts of solvent (w/v) in vials. Along with the 8 DESs, one precursor – i.e., octanoic acid – and reference solvents were tested for each wax, namely White Spirit for the beeswax and Ligroin 100–140 °C for the two microcrystalline waxes.

The vials were placed in a Vevor® digital ultrasonic cleaner (120 W, 50 Hz) to accelerate the solubilization process for 24 hours. The degree of solubilization was evaluated through turbidity measurements by filtering the mixture to remove solid residues. The analysis was performed using a Haze 3001 Turbidity Meter.

Contact angle measurements. Contact angle measurements were performed with the LAUDA Surface Analyzer LSA60 to assess the waxes' wettability using the tested formulations, thus evaluating the surface–liquid interactions. The eight DESs were examined, as well as reference solvents – i.e., White Spirit and Ligroin 100–140 °C – and deionized H_2O. The analysis was carried out by bringing down a drop of each solvent on microscope glass slides covered with 0.5 g of each wax. During the preparation of the mockups, the R21 dispersion was simply applied on the slides and let harden, while Beeswax and Renaissance® were slightly heated up to 50 °C to make them melt and form a flat and uniform surface. For each solvent–wax combination, three measurements were performed to reduce the uncertainty of the analysis. The results are presented as mean values.

Cleaning tests. Laboratory specimens were prepared by applying 0.5 g of each wax, both pure and mixed with the fluorescence marker Rhodamine 6G, on microscope glass slides to evaluate the solvents' solubility on an inert substrate. The waxes were loaded with Rhodamine 6G to allow for the evaluation of the effective removal of the wax layer in the treated areas through spectrocolorimetric analysis and multi-spectral imaging. Beeswax was heated up to 50 °C, while Renaissance® up to 40 °C to facilitate their application. Rhodamine 6G was added after the heating process. Once the solid state was reached, specimens were soaked in ethanol/water solution (20 : 70) for 3 hours to remove the excess marker, thus avoiding further extraction of the sole Rhodamine 6G during the cleaning tests. Swab cleaning tests were carried out simulating the operational mode commonly used by restorers: each solvent – also comprising reference solvents (i.e., White Spirit for beeswax and Ligroin 100–140 °C for microcrystalline waxes) – was left on the layers of wax in the same amount (1 mL) for increasing contact times – i.e., 1 minute, 2 minutes, and 3 minutes – and then the solvent's residues were removed from the surface using cotton swabs wounded on a thin stick. Tests were summarized in the Results section by assigning an average value to each wax–solvent combination. During the treatment, mechanical rubbing action was minimized to limit its contribution to the removal of the layer. Deionized water was

also used as a reference solvent, as it should not have any kind of interaction with wax. Spectrocolorimetric analyses were performed before and after the cleaning treatment using a portable spectrophotometer Y3060 3nh, equipped with a D65 illuminant and an 8 mm size aperture. The analysis was carried out in the SCI mode (Specular Component Included) and by measuring the spectra between 400 and 700 nm. The acquisitions were performed three times on each sample to reduce the uncertainty of the analysis. Data were then analyzed through the CIELab color system. The variation of the parameters L^*, a^* and b^* was calculated by evaluating the Euclidean distance between the mean of the values acquired on the areas after the treatment and the ones collected on the blank sample. ΔL^*, Δa^*, and Δb^* were summarized in the total color difference ΔE, given by the following equation:

$$\Delta E = \sqrt{(\Delta L^*)^2 + (\Delta a^*)^2 + (\Delta b^*)^2} \qquad (3)$$

For each sample, ΔE uncertainty was estimated through the calculation of the standard deviation of the ΔE_s computed for each triad of measurements. Smaller values indicate greater proximity of the treated area to the sample without the wax coating, thus demonstrating the higher effectiveness of the solvent. Higher values mean that the wax layer is still present to different degrees, hence proving the less interaction between the solvent and the wax.

Multispectral imaging was performed using UV (365 nm) and visible (VIS) light sources before and after the cleaning tests to evaluate the solvents' effectiveness. The analysis was carried out using the Madatec multispectral system, which consists of a full-spectrum Samsung NX500 Digital Camera (28.2 MP BSI CMOS) and Madatec spotlights with 365 nm (UV) wavelength. Images of the induced fluorescence were taken using the HOYA UV-IR filter cut 52 and the Yellow 495. 52 mm F-PRO MRC 022 filter to reduce the component of the UV spotlight, thus better highlighting possible fluorescence effects.[52] Fourier Transform Infrared (FT-IR) spectroscopy in the Attenuated Total Reflectance (ATR) mode was performed on the swabs used for the cleaning tests as well to further confirm the presence of the wax–solvent mixture on them, hence assessing the actual interaction between the solvent and the solute. The IR spectra were collected using the Nicolet Summit FTIR spectrometer equipped with the Everest™ Diamond ATR accessory. A total of 32 scans were performed on each sample with an instrumental resolution of 8 cm^{-1}.

Results

Solubility tests

Fig. 1 shows the dissolution degree of the waxes in the tested solvents. Total dissolution was not achieved with any of the tested DESs, including reference solvents that are commonly used for the removal of wax layers from works of art, namely Ligroin 100–140 °C for the microcrystalline waxes and White Spirit for the beeswax. Indeed, the interaction between the waxes and the solvents resulted in turbid colloidal dispersions
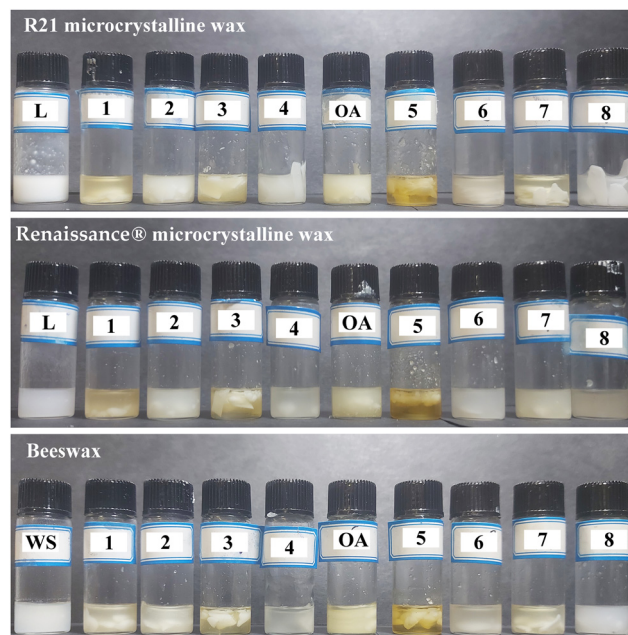

Fig. 1 Solubility tests, from the top to the bottom: R21 microcrystalline wax, Renaissance® microcrystalline wax, and beeswax mixed with the tested solvents in vials. L: ligroin 100–140 °C; octanoic acid: OA. DESs are labelled with consecutive numbering. Fatty acids-based DESs: 1, 2, 3, 7, 8; thymol-based DESs: 4, 5, 6.

instead of solutions. This effect is explained by the fact that the waxes form opaque colloidal systems in nonpolar organic solvents, by having particles with a size of few nanometers to 1 μm range.[53,54]

Due to the formation of colloidal dispersions, turbidity measurements were used to assess the degree of solubilization of the waxes in each solvent. High Nephelometric Turbidity Unit (NTU) values imply significant cloudiness of the mixture, meaning the formation of intermolecular interactions among the solvents and the waxes with the formation of the suspension. Conversely, low NTU values highlight a lack of interaction between the wax and the solvent. Fig. 2 illustrates the NTU values for each solvent–wax combination normalized to the reference solvents, i.e., Ligroin and White Spirit. The degree of dispersion of the microcrystalline wax R21 in each solvent can be defined as follows: L > DES 2 > DES 4 > O.A. > DES 6 > DES 3 > DES 1 > DES 8 > DES 5 > DES 7. As to the Renaissance® wax polish, turbidity measurements showed that: DES 2 > O.A. > DES 7 > L > DES 6 > DES 8 > DES 4 > DES 1 > DES 3 > DES 5. Fewer Deep Eutectic Solvents had the same dispersive effect on the beeswax, probably due to the presence of more polar groups in the beeswax chemical composition (complex wax esters, linear wax monoesters and hydroxy monoesters, free fatty acids, and free fatty alcohols).[55] The turbidity of the beeswax–solvent mixtures can be summarized as follows: WS > DES 8 > O.A. > DES 2 > DES 6 > DES 1 > DES 7 > DES 4 > DES 3 > DES 5.

Contact angle measurements

Contact angle measurements demonstrated the tendency of each solvent to spread over the surface or be repelled by it, thus
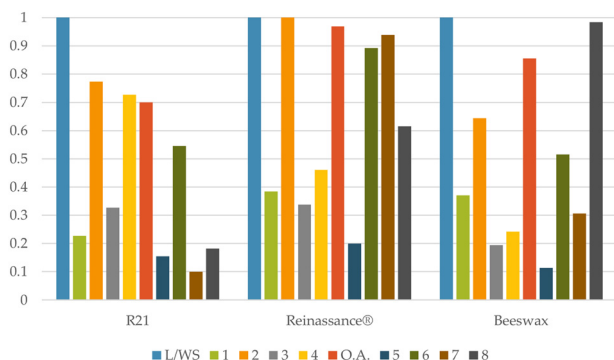
Fig. 2 Normalized values derived from turbidity measurements of solvent–wax mixtures. L: ligroin 100–140 °C (used as a reference for R21 and Renaissance®); WS: White Spirit (used as a reference for beeswax); octanoic acid: OA. DESs are labelled with consecutive numbering. Fatty acids-based DESs: 1, 2, 3, 7, 8; thymol-based DESs: 4, 5, 6.

defining the wettability of the three waxes by the tested DESs and references (Fig. 3). The poor wettability of the substrate by water is evidenced by the high contact-angle values, ranging from $91.4° \pm 1.5$ to $120° \pm 0.3$. On the other hand, the hydrophobicity of the reference solvents and DESs caused a high reduction of the contact angle values, highlighting the overall wettability of the three waxes by these formulations. As to the microcrystalline dispersion R21, the solvents showing the lower contact angle values, meaning the higher wettability, are as follows: WS, DES 4, DES 6, DES 2, and L, while higher values were acquired for DES 8, O.A., DES 7, DES 1, DES 3, DES 5. Results obtained from the analysis of Renaissance® wax showed similar results, even though outlining the general lower wettability by all the hydrophobic solvents, except for White Spirit. Indeed, only WS and DES 2 provided values lower than $20°$ – respectively $2.2° \pm 1.3$ and $19.9° \pm 1.6$. The results related to the other formulations can be summarized as follows (from the lower to the higher values): L, O.A., DES 8 = DES 6, DES 1, DES 7, DES 4, DES 3, DES 5.

Beeswax exhibited a general lower wettability by the tested solvents, whose contact-angle values are in the following order (from the lower to the higher one): WS, DES 2, DES 8, DES 1 = DES 7 = O.A., DES 6, DES 4, L, DES 3, DES 5.
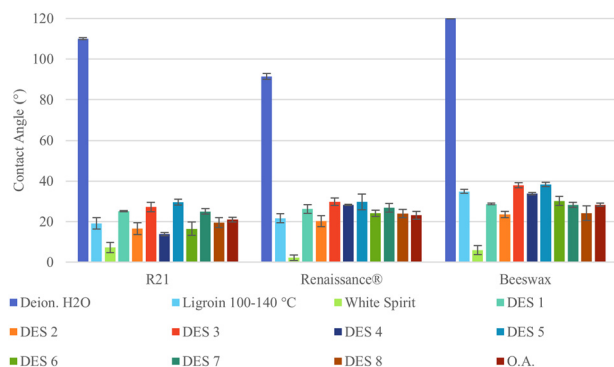
Cleaning tests

Spectrocolorimetric analysis. Table 2 reports the results of the spectrocolorimetric measurements, which enabled the definition of the DESs' cleaning performance on an inert substrate – *i.e.*, glass slides – hence assessing the effective removal of the coating by each solvent. The chromatic variation (ΔE) was calculated by comparing the chromatic values obtained after the cleaning tests with the ones of the microscope glass' (blank sample), thus describing the ability of the tested solvents in removing the wax. High ΔE values denote the presence of wax on the sample's surface, while low ones indicate the higher effectiveness of the solvent.

For R21, the solvents' efficacy based on spectrocolorimetric analysis can be defined as follows: L > DES 2 > DES 6 > DES 4 > DES 1 > DES 8 > DES 7 > O.A. > DES 3 > DES 5 > H$_2$. As to the Renaissance® wax polish, the results can be summarized as L > DES 2 > DES 4 > DES 7 > O.A. > DES 6 > DES 8 > DES 1 > DES 5 > DES 3 > H$_2$O. Finally, beeswax's ΔE values can be explained as WS > DES 2 > DES 8 > DES 1 > DES 7 > DES 4 > DES 6 > DES 5 > DES 3 > H$_2$O. The observations made during the removal of the wax layer, coupled with the results of the spectrocolorimetric measurements, enabled the definition of the cleaning performance on an inert substrate – *i.e.*, glass slides – hence assessing the effective removal of the coating by each solvent. As a general remark, longer contact times (*i.e.*, 3 minutes) allow for more efficient removal of the layer. Also, more hydrophobic DESs seem to interact with beeswax, while lesser with the microcrystalline wax R21. Indeed, beeswax is particularly responsive to DES 2 and 8, but also to DES 1, resulting in the following descending ranking: WS = DES 2 = DES 8, DES 1, DES 4 = O.A. = DES 7, DES 6, DES 3 = DES 5. The results obtained from the cleaning tests on Renaissance® can be summarized in descending order as L = DES 2, DES 4, O.A. = DES 7, DES 1 = DES 8, DES 3 = DES 5 = DES 6 while, as to R21, only DES 2 almost equals the result of the reference solvent (Ligroin). The other solvents appear to be able only to partially remove the wax layer, in the following descending sequence: L, DES 2, DES 1 = DES 4 = DES 6 = DES 8, DES 3 = O.A. = DES 7, DES 5. The

Fig. 3 Contact angle values: mean resulting from three measurements and standard deviation.

Table 2 Spectrocolorimetric parameter ΔE for each solvent–solute combination, resulting from the mean of three measurements. The standard deviation computed on ΔE_s is $0.47 <$ SD < 7.95

Solvent	$\Delta E^{\star}$ values		
	R21	Renaissance®	Beeswax
Deionized water	28.64	17.41	7.87
DES 1	13.66	16.02	3.06
DES 2	8.04	0.76	2.38
DES 3	24.21	16.77	7.01
DES 4	13.34	4.58	5.56
DES 5	27.01	16.76	7.00
DES 6	12.99	15.55	6.19
DES 7	22.86	9.96	5.34
DES 8	14.03	15.83	2.54
Ligroin/white spirit	4.44	0.63	2.33
Octanoic acid	23.67	10.46	5.69

Table 3 Average rating assigned during the cleaning tests. Legend: – stands for "no" removal", while ***** indicates complete removal of the wax layer

Solvent	R21	Renaissance®	Beeswax
Deionized water	–	–	–
Ligroin or white spirit	*****	*****	*****
DES 1	***	**	****
DES 2	****	*****	*****
DES 3	**	*	*
DES 4	***	****	***
Octanoic acid	**	***	***
DES 5	*	*	*
DES 6	***	*	**
DES 7	**	***	***
DES 8	***	**	*****

results reported in Table 3 summarize the outcome of the cleaning tests, expressed as an average rating based on the observations made during the removal considering the three different contact times.

Multispectral imaging. Multispectral imaging allowed showing the solvents' effectiveness in removing the waxes, supporting the observations made during the cleaning tests. The results obtained using three DESs – namely, DESs 1, 2, and 6 – are reported in Table 4 in both visible (VIS) and UV light, as an illustration of the different degrees of cleaning effectiveness defined in Tables 2 and 3. Furthermore, the differences given by the increasing contact times are visible in the pictures shown in Table 4. Thus, the results suggest the need for longer application times that are made possible by the negligible evaporation rate of the hydrophobic DESs, which also reflects their low impact on the operator, which is safeguarded from their inhalation.

FT-IR ATR. The presence of the wax–solvent mixture on the swabs used for the cleaning treatment was evaluated through FT-IR ATR. The analysis was performed on the swabs used for the cleaning tests to assess the presence of a mixture of the DESs and the waxes on all of them, thus confirming the actual formation of the colloidal dispersion during the cleaning treatment. The spectra were interpreted considering the peaks related to the presence of cellulose-based swabs, that were prior acquired as blank determination.

Indeed, the absorption band at 3391 cm^{-1} is assigned to hydroxyl groups stretching.[56] Bands at 2906 cm^{-1} and 1373 cm^{-1} are assigned to stretching and deformation vibrations of the C–H group that can be either related to the glucose unit of cellulose, the DESs, or the waxes (Fig. 4). The absorption band at 898 cm^{-1} is characteristic of β-glycosidic linkage between glucose units.

The signal at 1061 cm^{-1} is assigned to the –C–O– group of DESs' precursors and secondary alcohols or ethers functions existing in the cellulose chain backbone. Nevertheless, multiple peaks can be specifically attributed to the DESs or the wax, providing information about the dispersion of the substance.

As an example, the spectra acquired on the swabs used for the treatment of each type of wax with DES 1 are shown in Fig. 4–6.

Table 4 Multispectral imaging in VIS and UV (365 nm) lights showing the effects of DES 1, DES 2, and DES 6 on the three waxes based on the increasing contact times (1′, 2′, and 3′). SOL: solvent; RAD: radiation; R21: microcrystalline wax R21; RE: microcrystalline wax Renaissance®; BE: beeswax

As to the microcrystalline wax R21, the characteristic peaks at 725 cm^{-1} (C–H rocking of alkenes), 2850, and 2920 cm^{-1} (C–H stretching of alkenes) are visible in all the acquisitions,
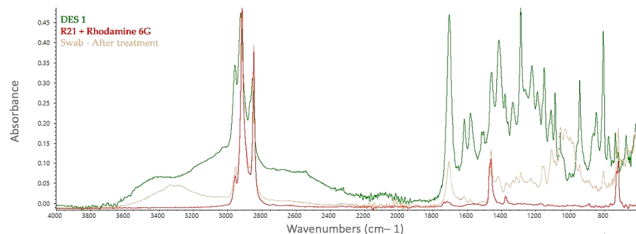
Fig. 4 FT-IR ATR spectra comparing DES 1, R21 mixed with Rhodamine 6G, and the swab used for the cleaning treatment.
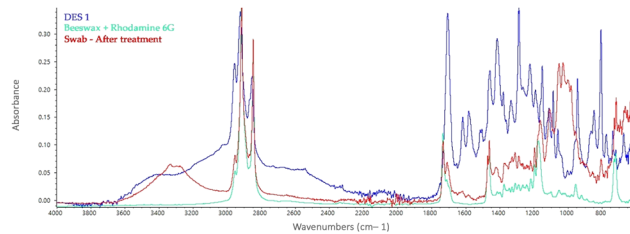

Fig. 6 FT-IR ATR spectra comparing DES 1, beeswax mixed with Rhodamine 6G, and the swab used for the cleaning treatment.

except for deionized water (Fig. 4).[57] At the same time, the peaks at 1720 cm^{-1} of C=O stretching of carboxylic acids, 1575 and 1620 cm^{-1} of C=C stretching of cyclic and conjugated alkenes, 1220 and 1290 cm^{-1} of C–O stretching, 815 cm^{-1} of C=C alkene bending can be associated with the solvent.

Due to the nature of the two microcrystalline waxes, the Renaissance® wax shows the same characteristic peaks as the R21 (Fig. 5). Hence, the same considerations can be made, also due the presence of the same bands related to the three DESs that can be seen in the previous spectra.

As to beeswax, the characteristic peaks at 2850 and 2920 cm^{-1} (C–H stretching of alkenes), 1740 cm^{-1} (C=O stretching of esters), 1460 cm^{-1} (C–H bending of alkanes), 1150 cm^{-1} (C–O stretching), 960 cm^{-1} and 725 cm^{-1} (C=C bending of alkenes) can be seen in the spectrum acquired on the swab after the treatment (Fig. 6) (Dubey, Sharma, & Kumar, 2017). Additionally, the peaks at 1720 cm^{-1} of C=O stretching of carboxylic acids, 1425 cm^{-1} of O–H bending, and 1150 cm^{-1} of C–O stretching are related to the solvent.

Discussion

The degree of dispersion of the waxes in the tested solvents was examined. The results showed that DES 2 and DES 4 produce a higher degree of dispersion on the microcrystalline wax R21, while DES 2, octanoic acid, and DES 7 showed the same good results in the dispersion of the microcrystalline wax Renaissance®. Also, DES 8, octanoic acid, and DES 2 effectively interacted with beeswax. However, it is worth mentioning that the degree of dispersion hinges not only on the affinity between the solvent and the dispersed phase but also on their relative proportion. The presence of solid residues of wax could be related to the oversaturation of the dispersion, thus suggesting

that complete dispersion of the wax can be obtained with a higher solvent volume. The R21-DES4, beeswax-DES2, beeswax-O.A., beeswax-DES8, and Renaissance®-DES2 mixtures were highly opaque, possibly entailing the saturation of the dispersion and, in the case of the R21-DES4, beeswax-DES2, and beeswax-O.A., leading to the formation of a semi-solid paste.

Contact angle measurements highlighted the general tendency of the DESs to spread onto the waxes' layers as opposed to deionized water, due to the higher affinity between the DESs and the solute having high hydrophobicity. Cleaning tests enabled the direct evaluation of the solvents' effectiveness by using the operating procedure commonly employed by restorers – i.e., the swab-cleaning method – thus providing valuable information on the DESs' actual potential for their use as new sustainable cleaning systems for the removal of non-polar substances from Cultural Heritage materials. The conclusions resulting from the cleaning tests, multispectral imaging, and spectrocolorimetry show that DES 2 almost equals the efficacy of Ligroin in removing the R21 microcrystalline wax, while DES 2 and DES 4 have a greater effect on the cleaning of the Renaissance® wax polish. In addition, DES 2, DES 8, and DES 1 were able to remove the beeswax layer successfully. Also, all the proposed formulations formed a semi-solid paste with the wax, allowing for easy removal of the solvent–solute mixture from the specimens' surface.

FT-IR ATR analyses confirmed the actual interaction between the solvent and the solute during the cleaning treatment, thus disproving the hypothesis that the removal of the layer may have been due to mechanical action. Indeed, the presence of both solvent and wax residues on the swabs used for the cleaning treatment showed that the agglomerated particles of the wax are effectively separated from each other through the action of the solvent.

Based on the whole study, it is possible to conclude that the combination L-(−)-menthol–cctanoic acid 1 : 1 (DES 2) shows a higher affinity with the three types of wax. Besides, promising results are also given by the application of DES 2 on the microcrystalline wax Renaissance® and by the utilization of dodecanoic acid–decanoic acid 1 : 2 (DES 8), followed by DES 2, and thymol–Decanoic acid 1 : 1 (DES 1) for the removal of beeswax.

The different solvent–solute interactions observed in the experimentation can be related to the different compositions of the three waxes. Indeed, microcrystalline waxes are produced
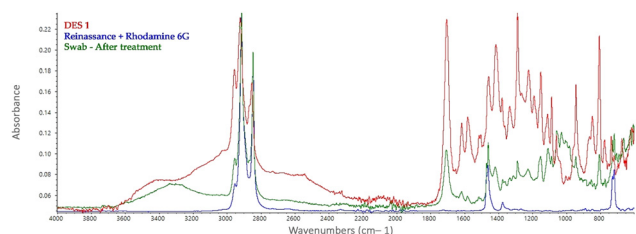

Fig. 5 FT-IR ATR spectra comparing DES 1, Renaissance® mixed with Rhodamine 6G, and the swab used for the cleaning treatment.

by de-oiling petrolatum, as part of the petroleum refining process. While paraffin wax contains mostly unbranched alkanes, microcrystalline wax is composed of a higher percentage of isoparaffinic (branched) hydrocarbons and naphthenic hydrocarbons.[56] Indeed, the presence of cyclic hydrocarbons in their composition explains the better dissolution of the microcrystalline wax R21 in DESs based on L-(−)-menthol. Their respective structures interact due to the formation of weak intermolecular forces involving the hydrophobic portions of the molecules – i.e., cyclic hydrocarbons. This phenomenon becomes particularly evident when DES 4 and DES 6 are compared. While DES 6 consists of equal proportions of L-(−)-menthol and thymol – containing an aromatic structure instead – DES 4 has twice as much L-(−)-menthol, thus causing greater dissolution of the solute.

Even though the Renaissance® wax polish is a microcrystalline wax as well, it does not contain naphthenic hydrocarbons. According to the information provided by producers, it is a mixture of waxes containing polyethylene wax – i.e., ultra-low molecular weight polyethylene based on ethylene monomer chains – which makes it more stable compared to other microcrystalline waxes intended for conservation.[58]

This difference in the composition between the two microcrystalline waxes may be the cause of their different interaction with the tested solvents. Octanoic acid seems to have greater compatibility with the Renaissance® wax, probably due to the chain length of low-molecular weight-based waxes. Indeed, low-molecular-weight waxes might have C8–C9 alkyl chains which could better interact with the alkyl chains of octanoic acid.

Even though differences have been pointed out between the two microcrystalline waxes, the intermolecular forces driving their interaction with the proposed solvents presumably consist of London dispersion forces involving the linear alkyl chains of the solvents – i.e., carboxylic acids – the branched hydrocarbons of the waxes, and the cyclic structures of both L-(−)-menthol and R21 microcrystalline wax.

Eventually, beeswax is a complex mixture of hydrocarbons (12–16%) with a predominant chain length of C27–C33, free fatty acids (12–14%), with a chain length of C24–C32, linear wax monoesters and hydroxy monoesters (35–45%) with chain lengths generally of C40–C48, complex wax esters (15–27%), and exogenous substances.[53] The presence of long alkyl chains, –OH, –COOR′, and –COOH groups in beeswax' structure explains the broad range of solubility of beeswax in low- and medium-polar solvents.[56] Also, the higher interaction between beeswax and DES 8 can be related to the presence of fatty acids having –COOH groups, similar to beeswax, and the longer alkyl chains among the tested acids. As to carboxylic-acids-containing DESs, the interaction between the solvents and beeswax can be mainly ascribed to the formation of hydrogen bonds between the polar moieties of the solvent and the beeswax. The carbonyl group –C=O of carboxylic acids can form hydrogen bonds with both the hydroxyl groups –O–H of fatty acids and wax hydroxy monoesters contained in the beeswax. Likewise, the hydroxyl group of the solvent can form hydrogen bonds with the carbonyl group of wax's fatty acids,

monoesters, and hydroxy monoesters. London dispersion forces play a significant role as well, by involving the hydrophobic moieties of the solvent and the solute. These interactions tend to increase with increasing the chain length, due to the higher number of electrons able to generate more instantaneous dipoles. Indeed, the reduction of the alkyl chain's length – as with octanoic acid-based and L-(−)-menthol or thymol-based DESs – the action on beeswax decreases, even though the hydroxyl groups should partially interact with the ones present in the wax.

Conclusions

The experimental process provided valuable results proving hydrophobic DESs' potential of being used as sustainable solvents for cleaning treatments on Cultural Heritage materials.

Hydrophobic Natural Deep Eutectic Solvents proved to be potentially suitable alternatives to more toxic organic solvents that are currently popular in the conservation of Cultural Heritage sector. Indeed, NADESs have low toxicity for the operator, as they consist of natural and biocompatible substances and have low volatility. This latter aspect has a twofold implication: a reduced amount of solvent is needed, since it does not evaporate and continues to interact with the coating to be removed as long as required, making the treatment fully sustainable; the operator does not inhale solvent vapors, thus avoiding health risks. Also, the low evaporation rate allows for the recovery of the DESs, which can be extracted from the solvent–solute mixture and reused. Several recycling methods are currently being studied for both hydrophilic and hydrophobic deep eutectic solvents – i.e., adsorption with activated carbon, back extraction, anti-solvent addition, crystallization, liquid–liquid extraction, solid–liquid extraction, short-path distillation, supercritical fluid extraction, membrane-based processes, and separation due to density and viscosity differences.[59–61] In addition, DESs have physical properties that make them suitable for use in cleaning operations, such as transparency, moderate viscosity, and effective interaction with the material to be removed.

In the present study, the potential of different NADES has been revealed. Specifically, L-(−)-menthol-based DESs–thymol/ L-(−)-menthol 1:2 in particular – provided positive results in combination with the R21 microcrystalline wax, presumably due to the presence of naphthenic hydrocarbons in the wax' composition. Octanoic acid-based DESs – i.e., L-(−)-menthol/ cctanoic acid 1:1 and dodecanoic acid/octanoic acid 1:3 – showed higher interaction with the Renaissance® wax, probably due to the alkyl chains' length of low-molecular-weight polyethylene waxes and branched hydrocarbons that may resemble that of octanoic acid. Eventually, fatty acid-based DESs with the longer alkyl chains – i.e., dodecanoic acid/ decanoic acid 1:2, L-(−)-menthol/octanoic acid 1:1 – show a greater affinity with beeswax due to the presence of the same –COOH functional groups and long alkyl chains in the structure of beeswax' constituents.

Future research will focus on the definition of the solubility parameters of hydrophobic deep eutectic solvents to determine the solubility parameters and the areas of the Teas Triangle in which they stand. The cleaning performance will be also evaluated on mockups reproducing Cultural Heritage works, such as stone and metal surfaces, examining once again the presence of solvent residues and the interaction between the hydrophobic NADESs and the substrate.

Author contributions

Chiara Biribicchi: conceptualization, methodology, data curation, writing – original draft preparation, visualization, investigation, writing – reviewing and editing, formal analysis. Andrea Macchia: conceptualization, methodology, data curation, writing – reviewing and editing, formal analysis, supervision, project administration. Gabriele Favero: validation, resources. Romina Strangis: resources. Bartolo Gabriele: resources. Raffaella Mancuso: resources, writing – original draft preparation. Mauro Francesco La Russa: project administration.

Conflicts of interest

There are no conflicts to declare.

Acknowledgements

Notes and references

1 B. Barclay and C. Hett, The Cleaning, Polishing, and Protective Waxing of Brass and Copper, *CGI Notes*, 2007, **9**, 3.

2 D. Comelli, G. Valentini, R. Cubeddu and L. Toniolo, Fluorescence Lifetime Imaging and Fourier Transform Infrared Spectroscopy of Michelangelo's David, *Appl. Spectrosc.*, 2005, **59**, 1174–1181.

3 T. J. Shedlosky, K. M. Stanek and G. Bierwagen, in *AIC Objects Speciality Group Postprints*, 2000, vol. 320, pp. 452–9545.

4 L. Robbiola, C. Fiaud and S. Pennec, in ICOM Committee for Conservation Tenth Triennal Meeting, Washington DC, 1993, p. 911.

5 E. Vara Fabjan, T. Kosec, V. Kuhar and A. Legat, *Mater. Technol.*, 2011, **45**, 585–591.

6 O. Seung-Jun and W. Koang-Chul, *J. Korea Convergence Soc.*, 2018, **9**, 151–160.

7 M. Toro, T. Beentjes, I. Joosten, J. Bloser and L. Zycherman, in Metal 2019 – Interim Meeting of the ICOM-CC Metals Working Group, Neuchatel, 2019.

8 B. Salvadori, D. Pinna and S. Porcinai, *Environ. Sci. Pollut. Res.*, 2014, **21**, 1884–1896.

9 D. E. Couture-Rigert, P. J. Sirois and E. A. Moffatt, *Stud. Conserv.*, 2012, **57**, 142–163.

10 S. Barreca, M. Bruno, L. Oddo and S. Orecchio, *Nat. Prod. Res.*, 2019, **33**, 947–955.

11 V. M. Pozhidaev, V. M. Retivov, A. V. Kamaev, S. K. Belus, A. S. Nartov, V. A. Rastorguev, I. V. Borodin, E. Y. Tereschenko, R. A. Sandu, E. B. Yatsishina and M. V. Kovalchuk, *Heritage Sci.*, 2019, **7**, 90.

12 L. Kubick and J. Giaccai, *AIC Objects Specialty Group Postprints*, 2012, 19, pp. 45–69.

13 G. D'Ercoli, M. Marabelli, V. Santin, A. Buccolieri, G. Buccolieri, A. Castellano and G. Palamà, *9th International Conference on NDT of Art*, Jerusalem, 2008.

14 I. M. Marcelli and M. Mercalli, in *9th International Conference on NDT of Art*, Jerusalem, 2008.

15 J. Wolfe, R. Grayburn, H. Khanjian, A. Heginbotham and A. Phenix, *ICOM-CC 18th Triennial Conference*, Copenhagen, 2017.

16 E. Risser and D. Saunders, *The restoration of ancient bronzes: Naples and beyond*, Getty Publications, Los Angeles, 2013.

17 U. Knutinen and A. Norman, *15th World Conference on Nondestructive Testing*, Rome, 2000.

18 N. Swartz and T. L. Clare, *J. Am. Inst. Conserv.*, 2015, **54**, 181–201.

19 O. Seung-Jun and W. Koang-Chul, *J. Conserv. Sci.*, 2017, **33**, 121–130.

20 G. Cavallaro, S. Milioto and G. Lazzara, *Langmuir*, 2020, **36**, 3677–3689.

21 C. Lim, *Collections Care: Staying Relevant in Changing Times, ASEAN & Beyond*, Singapore, 2019.

22 S. Kezic, J. Kruse and I. Jakasa, *Review of dermal effects and uptake of petroleum hydrocarbons*, 2010.

23 S. Parasuraman, W. Ping, P. Raj, J. Sujithra, B. Syamittra, W. Yeng, S. Dhanaraj and S. Muralidharan, *J. Basic Clin. Pharm.*, 2014, **5**, 89.

24 M. A. Amoruso, J. F. Gamble, R. H. McKee, A. M. Rohde and A. Jaques, *Int. J. Toxicol.*, 2008, **27**, 97–165.

25 V. Ferrara, A. Macchia and S. Sapia, in *Proceedings of 2013 Digital Heritage International Congress*, ed. A. C. Addison, L. de Luca, G. Guidi and S. Pescarin, 2013, pp. 409–412.

26 D. Dagostino, A. Macchia, R. Cataldo, L. Campanella and A. Campbell, *Int. J. Archit. Heritage*, 2015, **9**, 290–299.

27 P. T. Anastas and J. C. Warner, *Green Chemistry: Theory and Practice*, Oxford University Press, Oxford, 1998.

28 A. Macchia, H. Aureli, F. Prestileo, F. Ortenzi, S. Sellathurai, A. Docci, E. Cerafogli, I. A. Colasanti, M. Ricca and M. F. la Russa, *Methods Protoc.*, 2022, **5**(3), 37.

29 A. Macchia, C. Biribicchi, P. Carnazza, S. Montorsi, N. Sangiorgi, G. Demasi, F. Prestileo, E. Cerafogli, I. A. Colasanti, H. Aureli, M. Zappelli, M. Ricca and M. F. la Russa, *Sustainability*, 2022, **14**(7), 3972.

30 A. Macchia, H. Aureli, C. Biribicchi, A. Docci, C. Alisi, F. Prestileo, F. Galiano, A. Figoli, R. Mancuso, B. Gabriele and M. F. la Russa, *Materials*, 2022, **15**(16), 5671.

31 L. Randazzo, M. Ricca, D. Pellegrino, D. la Russa, A. Marrone, A. Macchia, L. Rivaroli, F. Enei and M. F. la Russa, *Int. J. Conserv. Sci.*, 2020, **11**, 243–250.

32 A. Macchia, O. Bettucci, E. Gravagna, D. Ferro, R. Albini, B. Mazzei and L. Campanella, *J. Nanomater.*, 2014, **2014**, 167540.

33 T. E. Achkar, H. Greige-Gerges and S. Fourmentin, *Environ. Chem. Lett.*, 2021, **19**, 3397–3408.

34 E. L. Smith, A. P. Abbott and K. S. Ryder, *Chem. Rev.*, 2014, **114**, 11060–11082.

35 C. Florindo, L. C. Branco and I. M. Marrucho, *ChemSusChem*, 2019, **12**, 1549–1559.

36 C. Florindo, L. Romero, I. Rintoul, L. C. Branco and I. M. Marrucho, *ACS Sustainable Chem. Eng.*, 2018, **6**, 3888–3895.

37 B. D. Ribeiro, C. Florindo, L. C. Iff, M. A. Z. Coelho and I. M. Marrucho, *ACS Sustainable Chem. Eng.*, 2015, **3**, 2469–2477.

38 Y. Jia, G. Sciutto, A. Botteon, C. Conti, M. L. Focarete, C. Gualandi, C. Samorì, S. Prati and R. Mazzeo, *J. Cult. Herit.*, 2021, **51**, 138–144.

39 A. Macchia, R. Strangis, S. de Angelis, M. Cersosimo, A. Docci, M. Ricca, B. Gabriele, R. Mancuso and M. F. la Russa, *Materials*, 2022, **15**(11), 4005.

40 N. Schaeffer, M. A. R. Martins, C. M. S. S. Neves, S. P. Pinho and J. A. P. Coutinho, *Chem. Commun.*, 2018, **54**, 8104–8107.

41 C. C. Fernandes, R. Haghbakhsh, R. Marques, A. Paiva, L. Carlyle and A. R. C. Duarte, *ACS Sustainable Chem. Eng.*, 2021, **9**, 15451–15460.

42 D. J. G. P. van Osch, C. H. J. T. Dietz, J. van Spronsen, M. C. Kroon, F. Gallucci, M. van Sint Annaland and R. Tuinier, *ACS Sustainable Chem. Eng.*, 2019, **7**, 2933–2942.

43 F. D. Dick, *Occup. Environ. Med.*, 2006, **63**, 221–226.

44 P. Makoś, A. Przyjazny and G. Boczkaj, *J. Chromatogr. A*, 2018, **1570**, 28–37.

45 R. Wang, D. Sun, C. Wang, L. Liu, F. Li and Z. Tan, *Sep. Purif. Technol.*, 2019, **215**, 102–107.

46 D. Ge, Y. Zhang, Y. Dai and S. Yang, *J. Sep. Sci.*, 2018, **41**, 1635–1643.

47 M. A. R. Martins, L. P. Silva, N. Schaeffer, D. O. Abranches, G. J. Maximo, S. P. Pinho and J. A. P. Coutinho, *ACS Sustainable Chem. Eng.*, 2019, **7**, 17414–17423.

48 M. Tiecco, F. Cappellini, F. Nicoletti, T. del Giacco, R. Germani and P. di Profio, *J. Mol. Liq.*, 2019, **281**, 423–430.

49 O. G. Sas, M. Castro, Á. Domínguez and B. González, *Sep. Purif. Technol.*, 2019, **227**, 115703.

50 K. Li, Y. Jin, D. Jung, K. Park, H. Kim and J. Lee, *J. Chromatogr. A*, 2020, **1614**, 460730.

51 F. Bergua, M. Castro, C. Lafuente and M. Artal, *J. Mol. Liq.*, 2022, **368**, 120789.

52 A. Macchia, C. Biribicchi, L. Rivaroli, H. Aureli, E. Cerafogli, I. A. Colasanti, P. Carnazza, G. Demasi and M. F. la Russa, *Methods Protoc.*, 2022, **5**(3), 52.

53 L. Ivanovszky, Waxes: Colloidal Properties and Systems, *J. Polym. Sci.*, 1962, **58**, 273–288.

54 J. M. Coulson, R. K. Sinnott and J. F. Richardson, *Coulson & Richardson's Chemical Engineering – Volume 2A: Particulate Systems and Particle Technology*, Butterworth-Heinemann, Oxford, 2019, pp. 693–737.

55 F. Fratini, G. Cilia, B. Turchi and A. Felicioli, *Asian Pac. J. Trop. Med.*, 2016, **9**, 839–843.

56 M. Aqil, B. Abderrahim, E. Abderrahman, A. Mohamed, T. Fatima, T. Abdesselam and O. Krim, *World J. Environ. Eng.*, 2015, **3**, 95–110.

57 P. Dubey, P. Sharma and V. Kumar, *Data Brief*, 2017, **15**, 615–622.

58 C. v Horie, *Materials for Conservation*, Routledge, Abingdon, 2010.

59 A. Isci and M. Kaltschmitt, *Biomass Convers. Biorefin.*, 2022, **12**, 197–226.

60 C. Florindo, F. Lima, L. C. Branco and I. M. Marrucho, *ACS Sustainable Chem. Eng.*, 2019, **7**, 14739–14746.

61 W. Zhu, P. Jin, M. Cheng, H. Yang, M. Du, T. Li, G. Zhu and J. Fan, *Talanta*, 2021, **233**, 122523.